Vietnam Journal of Science and Technology ***62*** *(3) (2024) 453-462*

doi:10.15625/2525-2518/16311

Synthesizing and investigating the electrical properties of carbonized metal–organic frameworks

Huy Quoc Tran[1], Huong Thi Diem Nguyen[2], Hoang Van Nguyen[2], Nhung Thi Tran[1], Tung Thanh Nguyen[3], Long Hoang Ngo[3], Thach Ngoc Tu[4, *]

[1]*HCMC University of Technology and Education, 01 Vo Van Ngan Street, Thu Duc District, Ho Chi Minh City, Viet Nam*

[2]*University of Science, Vietnam National University (VNU-HCM), 227 Nguyen Van Cu street, district 5, Ho Chi Minh city, Viet Nam*

[3]*NTT Hi-Tech Institute, Nguyen Tat Thanh University, 300A Nguyen Tat Thanh Street, District 4, Ho Chi Minh City, Viet Nam*

[4]*Nguyen Tat Thanh University, 300A Nguyen Tat Thanh Street, District 4, Ho Chi Minh City, Viet Nam*

[*]Emails: *tnthach@ntt.edu.vn*

Received: 21 July 2021; Accepted for publication: 9 February 2024

Abstract. The metal–organic frameworks (MOFs)such as VNU-20, ZIF-8, ZIF-67, MOF-199, and MIL-53 were synthesized and carbonized. The obtained MOFs and their carbonized analogs were characterized by powder X-ray diffraction. Subsequently, the carbonized materials were mixed with poly(vinylidene fluoride-*co*-hexafluoroproplylene)/(1-Methyl-2- Pyrrolidinone) at 5 wt% and cast on glassy carbon electrodes for subsequent analyses. The cyclic voltammetry (CV) measurements of carbonized samples were carried out. The resulting CV scans indicate the reversible CV curves of carbonized VNU-20 electrodes through the reversible redox oxidation reactions between Fe^{II} and Fe^{III}. Alongside this, the carbonized VNU-20 is found to have a comparable capacitance with that of carbonized ZIF-67, which is among the highest capacitance materials recorded in the literature for the same class of materials. Although further experiments need to be carried out for the optimization, our analysis initially reveals the promising properties of the carbonized VNU-20 electrode for electro-catalysis and the supercapacitor.

Keywords: Metal organic framework, carbonization, electrode, electrocatalysis, supercapacitor.

Classification numbers: 2.4.4, 2.10.1, 2.8.2

1. INTRODUCTION

Metal-organic frameworks (MOFs) belong to the new class of porous materials. The structure of MOFs is constructed based on the reticular chemistry, for which the selection of building blocks results in various crystal architectures with adjustable pore sizes, shapes, and tunable internal chemical environments [1 - 3]. The high porosity of MOFs, on which the pore sizes and shapes are tunable with functional groups, makes this material obtain advanced

properties over traditional materials. Due to those characteristics, they are applied in many different fields [4 - 8].

Recently, the need for mobile electrochemical energy storage devices with high capacity has been strongly researched and developed. In the early 1990s, the US Department of Energy set up a great deal of battery research and supercapacitors, i.e. storage models between batteries (low power/ high energy) and capacitors (high power/ low energy), which raises international awareness of supercapacitors [9]. Specifically, the structure of the supercapacitor consists of two electrodes (symmetrical or asymmetrical), electrolyte, and the diaphragm. Depending on the charge storage mechanism of the supercapacitor, there are two kinds of mechanisms that can be listed: electrical double-layer and pseudo-capacitor. While energy storage in an electrical double-layer is based on a physical process with the ability of charges to dissociate ions from the electrolyte at the transition layer, the charge storage mechanism of pseudo-capacitor with the rapid and reversible redox reactions takes place on the surface of the pseudo-capacitor electrodes. The electrolyte acts as the ion conductor for the supply of counter ions to fulfill the half-reactions on both electrodes [10 - 12].

For these reasons, a vast number of researches have been performed to enhance the power and energy storage of supercapacitors. This leads to the invention of novel electrolytes or electrode materials [13]. Among viable directions, the carbon-metal oxide composite synthesized from carbonization of MOFs, zeolitic imidazolate frameworks (ZIFs) exhibit the potential as the electrode materials because of high conductivity and surface area, which supports the fast diffusion of the ions from the electrolyte as well as the high density of metal centers spreading onto the internal surface of the materials, which are viable for redox reactions [14 - 18]. Since the nature of MOFs, ZIFs materials composed of a variety of structures with different metal oxide clusters and organic linkers, it was found vitally for screening among the MOFs, ZIFs and their carbonized analogues to choose the suitable materials, which achieved the balance between the porosity, conductivity as well as the tunability between the oxidation states.

Herein, the iron-based Metal–organic framework (Fe-MOF), VNU-20 [19], and its carbonized analogues were synthesized to investigate the electrical properties. Furthermore, other materials such as ZIF-8, ZIF-67, MOF-199, MIL-53, and their carbonized analogues were also synthesized for comparison [20 - 22]. The initial experiments show promising results with the reversible redox switching between Fe(II) and Fe(III) shown by the cyclic voltammetry curve of the carbonized VNU-20 samples. Furthermore, the electrode composed of carbonized VNU-20 shows a comparable capacitance to that of carbonized ZIF-67, a material with the highest capacitance recorded up to date for the class of carbonized MOF, ZIF materials [23]. While further experiments need to be carried out for the optimization, initial analyses showed promising result for further investigation and use of carbonized VNU-20 as the electrode material for electro-catalysis and the supercapacitor.

2. MATERIALS AND METHODS

2.1. Materials

Teraphthalic acid (H_2BDC, 98 % purity), 2-methylimidazole (MIM, 99 % purity), trimesic acid (H_3BTC, 95 % purity), 2,6–naphthalene dicarboxylic acid (H_2NDC, 95 % purity), $FeCl_2$ (anhydrous, 98 % purity), $Co(NO_3)_2{\cdot}6H_2O$ (98 % purity), $Cu(NO_3)_2{\cdot}3H_2O$ (98 % purity) were purchased from Sigma Aldrich Co., dimethylformamide (DMF, 99 % purity), dichloromethane (CH_2Cl_2, 99.5 % purity), methanol (MeOH, 99.8 % purity), ethanol (EtOH, 99.5 % purity) were

purchased from Acros Co., polytetrafluoroethylene (PTFE, 60 wt% in water) was purchased Sigma Aldrich Co. All of the starting materials were used without purification.

2.2. Methods

Synthesis of VNU-20. A mixture of 2,6-naphthalenedicarboxylic (0.09 g), trimesic acid (0.03 g) and $FeCl_2$ (0.09 g) were weighed into a reaction vial. Subsequently, DMF (5 ml) was added and the reaction mixture was sonicated for 10 minutes and placed in a pre-heating oven at 200 ºC for 72 h. Following this, the solid crystal was collected, washed, and exchanged with DMF (5 × 5 ml), MeOH (5 × 5 ml). The solid product was then activated under the dynamic vacuum for 12 h at 80 °C to obtain VNU-20 [19].

Synthesis of MIL-53. Terephthalic acid (0.1661 g) and $FeCl_3 \cdot 6H_2O$ (0.2702 g) were weighed into a reaction vial. Subsequently, DMF (5 ml) was added and the reaction mixture was sonicated for 10 minutes and placed in a pre-heating oven at 150 ºC for 24 h. Following this, the solid precipitate was collected by centrifugation, washed, and exchanged with DMF (5 × 5 ml), MeOH (5 × 5 ml). The solid product was then activated under the dynamic vacuum for 12 h at 80 ºC to obtain activated MIL-53 [21].

Synthesis of ZIF-8. 2-methylimidazole (0.0168 g) and $Zn(NO_3)_2 \cdot 6H_2O$ (0.067 g) were weighed into a reaction vial. Subsequently, DMF (5 ml) was added and the reaction mixture was sonicated for 10 minutes and placed in a pre-heating oven at 120 ºC for 24 h. Following this, the solid crystal was collected, washed, and exchanged with DMF (5 × 5 ml), MeOH (5 × 5 ml). The solid product was then activated under the dynamic vacuum for 12 h at 80 ºC to obtain activated ZIF-8 [20].

Synthesis of ZIF-67. 2-methylimidazole (0.1642 g) and $Co(NO_3)_2 \cdot 6H_2O$ (0.194 g were weighed into a reaction vial. Subsequently, the solvent mixture of DMF (3.5 ml) and ethanol (1.5 ml) were added. The reaction mixture was then sonicated for 10 minutes and placed in a pre-heating oven at 120 ºC for 24 h. Following this, the solid crystal was collected, washed and exchanged with DMF (5 × 5 ml), MeOH (5 × 5 ml). The solid product was then activated under the dynamic vacuum for 12 h at 80 ºC to obtain activated ZIF- 67 [20].

Synthesis of MOF-199. The mixture of trimesic acid (0.1764 g) and $CuCl_2 \cdot 2H_2O$ (0.23256 g) were weighed into a reaction vial. Subsequently, the solvent mixture of DMF (1.67 ml)/Ethanol (1.67 ml)/H_2O (1.67 ml) was added. The reaction mixture was then sonicated for 10 minutes and placed in a pre-heating oven at 85 ºC for 24 h. After that, the solid crystal was collected, washed and exchanged with DMF (5 × 5 ml), MeOH (5 × 5 ml). The solid product was then activated under dynamic vacuum for 12 h at 80 ºC to obtain MOF-199 [22].

Carbonization of MOFs. The materials were carbonized at an investigated temperature under the inner atmosphere. In detail, the obtained MOF material (~ 70 mg) was spread onto the glass slide (2 × 8 cm) and placed in a glass tube (2.5 × 30 cm). The glass tube was then placed in an oven and purged with N_2 for 5 minutes, followed by heating up to the desired temperature.

Preparation of Electrode. The carbonized MOF samples (10 mg) were ground for 10 minutes. Subsequently, PVDF-HFP/NMP (Poly(Vinylidene fluoride-co-hexafluoroproplylene) /(1-Methyl-2- Pyrrolidinone)) (5 % PVDF-HPF) (10.5 µl) was added as a binder. The mixture was then dispersed in 0.5 ml acetone. Following this, the obtained colloidal solution (50 µl) was coated on a working electrode and placed in a pre-heated oven at 80 ºC for 30 minutes. The sample weight was then calculated based on the amount of taken solution (0.5 ml acetone) with the assumption of homogenous dispersions.

Cyclic voltammetry analysis (CV). The electrochemical properties of carbonized MOFs and ZIFs were investigated by the CV analysis method using a standard three-electrode setup with Li_2SO_4 (30 ml, 2M) as the electrolyte, platinum (Pt) as the counter electrode, Ag/AgCl as the reference electrode and glassy carbon as the working electrode.

Calculation of Capacitance. The capacitances are calculated using the below equation, in which, C is the capacitance (F g^{-1}); ∫IdV is the area below the CV curve at the redox peaks positions; m is the sample mass (g); ν is the scanning rate (mV s^{-1}), ΔV is scanning window chosen based on redox peaks positions.

$$C = \frac{\int IdV}{m * v * \Delta V}$$

PXRD measurement. Powder X-ray data were collected using a Bruker D8 Advance Eco employing Ni filtered Cu Kα (λ = 1.54178 Å). The system was also outfitted with an anti-scattering shield that prevents incident diffuse radiation from hitting the detector. Samples were placed on zero background sample holders by dropping powders from a spatula and then leveling the sample with a spatula. The 2θ range was 3 - 50° with a step size of 0.02° and a fixed counting time of 0.5 s/step.

3. RESULTS AND DISCUSSION

3.1. Materials synthesis and carbonization

Synthesis and carbonization of VNU-20. The activated sample of VNU-20 was analyzed by powder X-ray diffraction (PXRD). The resulted patterns confirmed that pure VNU-20 has been obtained (Figure 1a). The slight differences in intensity were attributed to the orientation of the crystal during diffraction analysis [19]. Subsequently, the activated VNU-20 samples were carbonized at three different temperatures (400, 500 and 600 ºC) for three hours. The PXRD patterns of the carbonized samples have been collected (Figure 1b). The results indicated the decomposition of VNU-20 when increasing temperature and completely transforming into oxide at 600 ºC.

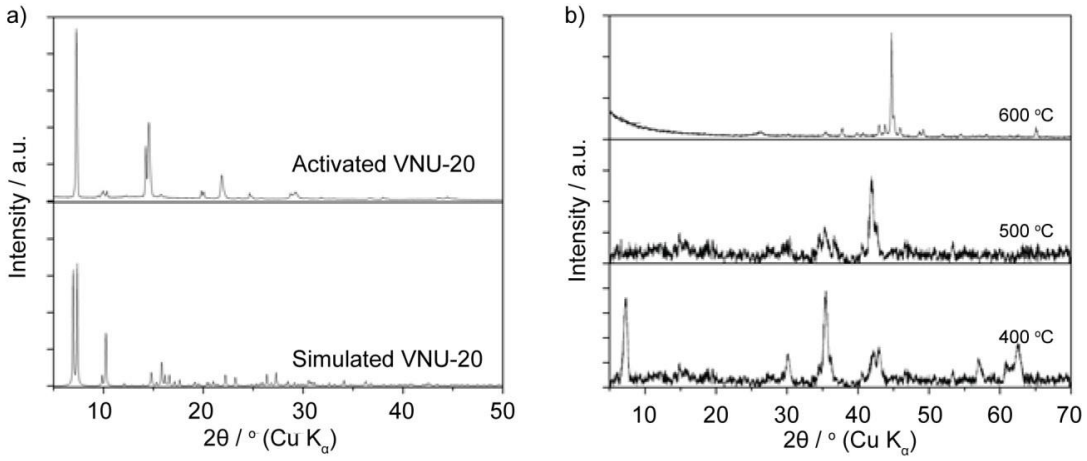

Figure 1. a) Powder X-ray diffraction pattern of activated VNU-20 in comparison with a simulated one. b) Powder X-ray diffraction pattern of carbonized VNU-20 at different temperatures.

Synthesis and carbonization of MIL-53. The activated sample of MIL-53 was analyzed by powder X-ray diffraction (PXRD). The resulted patterns confirmed that pure MIL-53 has been obtained (Figure 2a). The slight difference in diffraction patterns was attributed to the flexible nature of MIL-53 structure and was observed previously in the literature [24]. Similarly, the activated MIL-53 samples were carbonized at three different temperatures (400, 500 and 600 ºC) for three hours. The PXRD patterns of the carbonized samples have been collected (Figure 2b). The results indicated the complete transformation of MIL-53 to Fe_3O_4 (peaks at 2θ = 24, 33, 36 º) at 600 ºC.

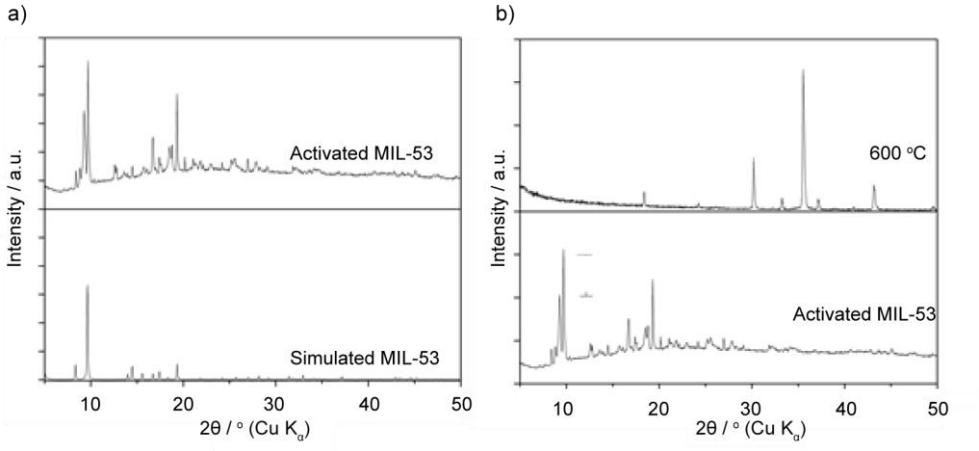

Figure 2. a) Powder X-ray diffraction pattern of activated MIL-53 in comparison with a simulated one. b) Powder X-ray diffraction pattern of carbonized MIL-53 at 600 ºC.

Synthesis and carbonization of ZIF-8. The activated sample of ZIF-8 was analyzed by powder X-ray diffraction (PXRD). The resulted patterns confirmed that pure ZIF-8 has been obtained (Figure 3a). The activated ZIF-8 samples were carbonized at three different temperatures (400, 500 and 600 ºC) for three hours. The PXRD patterns of the carbonized samples have been collected (Figure 3b). The results indicated the partial transformation of ZIF-8 to ZnO (peaks at 2θ = 32, 35, 37º) at 600 ºC.

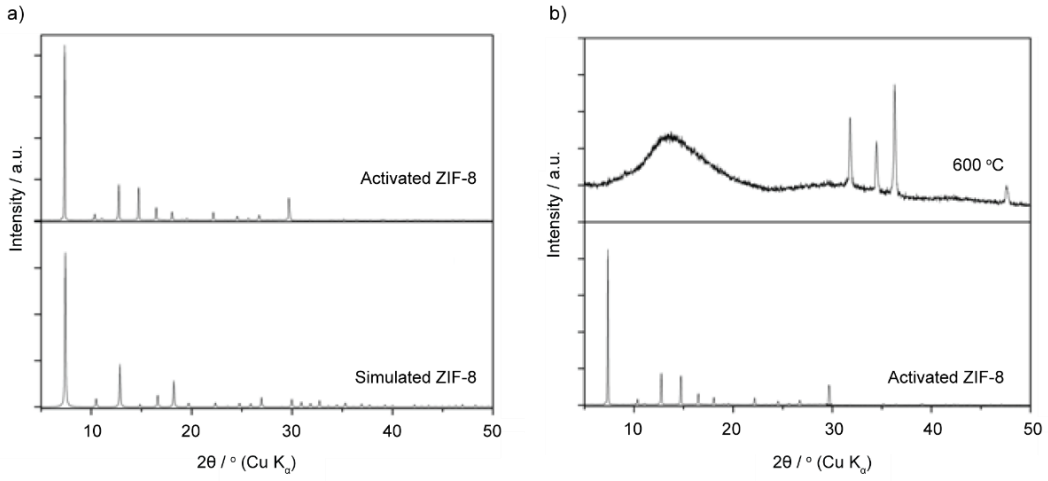

Figure 3. a) Powder X-ray diffraction pattern of activated ZIF-8 in comparison with a simulated one. b) Powder X-ray diffraction pattern of carbonized ZIF-8 at 600 ºC.

Synthesis and carbonization of ZIF-67. The activated sample of ZIF-67 was analyzed by powder X-ray diffraction (PXRD). The resulted patterns confirmed that pure ZIF-67 has been obtained (Figure 4a). The slight differences in intensity were attributed to the orientation of the crystal during diffraction analysis. The activated ZIF-67 samples were carbonized at three different temperatures (400, 500 and 600 ºC) for three hours. The PXRD patterns of the carbonized samples have been collected (Figure 4b). The results indicated the decomposition of ZIF-67 to transform into an amorphous phase at 600 ºC.

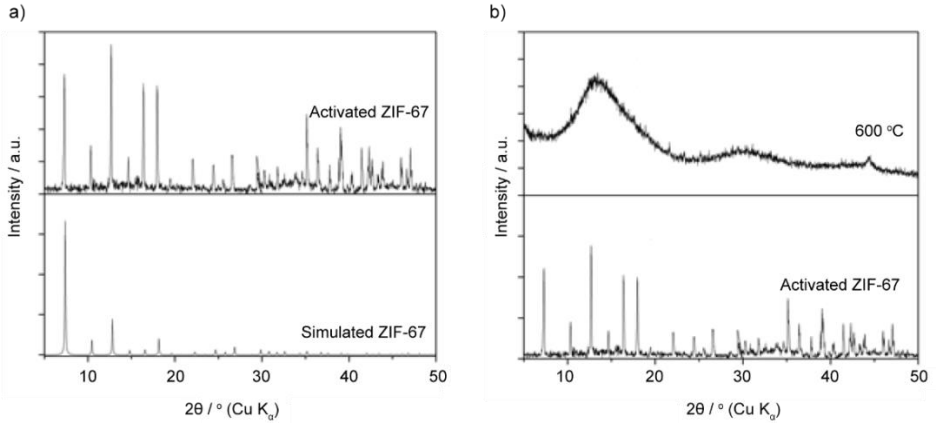

Figure 4. a) Powder X-ray diffraction pattern of activated ZIF-67 in comparison with a simulated one. b) Powder X-ray diffraction pattern of carbonized ZIF-67 at 600 ºC.

Synthesis and carbonization of MOF-199. The activated sample of MOF-199 was analyzed by powder X-ray diffraction (PXRD). The resulted patterns confirmed that pure MOF-199 has been obtained (Figure 5a). The activated MOF-199 sample was carbonized at three different temperatures (400, 500 and 600 ºC) for three hours. The PXRD patterns of the carbonized samples have been collected (Figure 5b). The results indicated the decomposition of MOF-199 to transform into CuO phase (peaks at 2θ = 32, 35, 37 º) at 600 ºC.

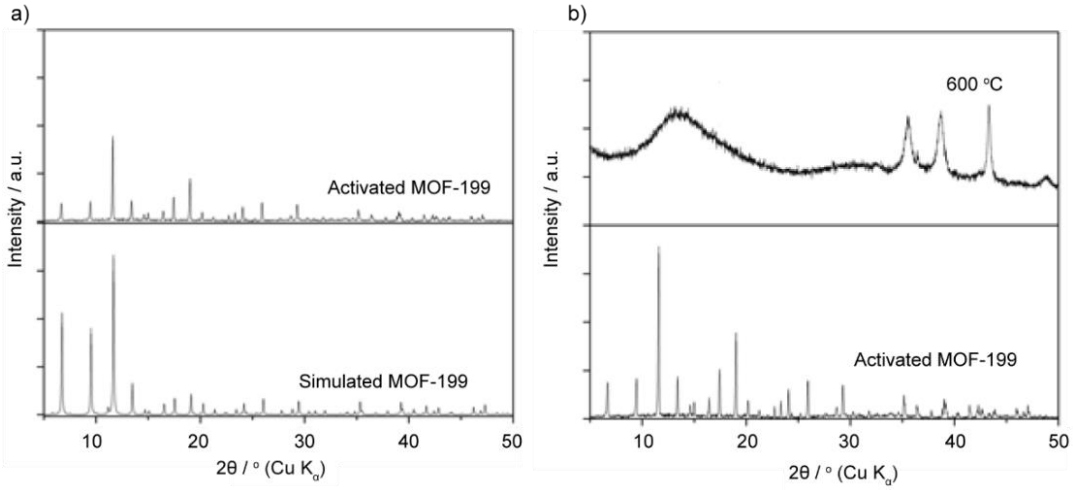

Figure 5. a) Powder X-ray diffraction pattern of activated MOF-199 in comparison with a simulated one. b) Powder X-ray diffraction pattern of carbonized MOF-199 at 600 ºC.

3.2. Investigation and discussion on characteristics of the electrical properties of carbonized MOFs

We initially investigated the electrical properties of carbonized samples of VNU-20 at three different temperatures using the cyclic voltammetry analysis (CV) method. We found that carbonization of VNU-20 at 400 and 500 ºC resulted in oxide with broad oxidation peaks (from -0.9 to -0.55; -0.5 to 0.15 V) and reduction peaks (from -0.5 to -0.75 V) while carbonization at 600 ºC (termed VNU-20-600) resulted in the different shape of the CV curve with the appearance of broad oxidation peaks (-0.25 to -0.11; 0.3 to 0.55) and reduction peak (from 0.4 to 0.25; -0.2 to -0.35 V) as well as the significant increase of current density. Furthermore, since the CV curve of VNU-20-600 is similar to that of activated carbon, it implied that the carbon-oxide composite successfully forms and helped increase the capacitance of resulted carbonization materials.

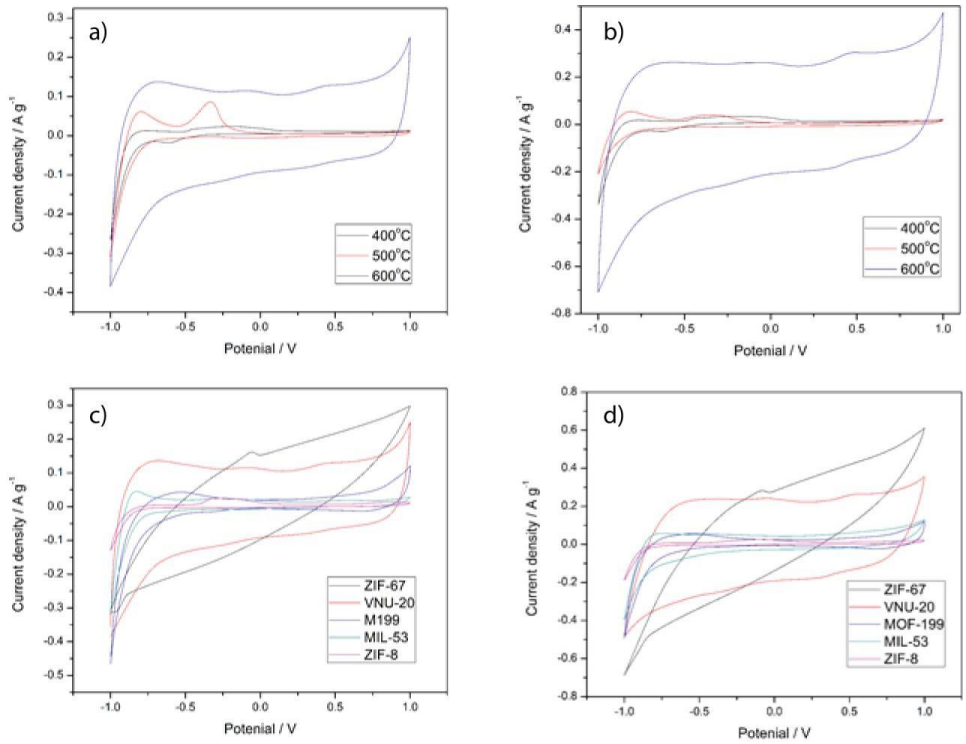

Figure 6. Cyclic voltammetry analysis of carbonized VNU-20 at three different temperatures with a scan rate of (a) 20 mV/s and (b) 50 mV/s. Cyclic voltammetry analysis of different carbonized MOFs and ZIFs with a scan rate of (c) 20 mV/s and (d) 50 mV/s.

We further investigated the electrical properties of different carbonized MOFs and ZIFs (Figure 6). Accordingly, the carbonization of ZIF-67 at 600 °C (ZIF-67-600) resulted in an amorphous phase (Figure 4) with broad oxidation peaks (from 0.15 to -0.05 V) while an unclear reduction peak was observed. The CV profile of ZIF-67-600 with large hysteresis, is similar to that of activated carbon implying the successful formation of the carbon-oxide composite. On the opposite, the ZIF-8-600 sample showed a broad oxidation peak from -0.4 to 0.25 V with a much lower current density compared to that of carbonized ZIF-67 and VNU-20. Moreover, the CV analysis of the other carbonized samples, MIL-53-600 and MOF-199-600 were also shown with a low current density as well as an unclear redox peak.

4. CONCLUSIONS

An iron-based Metal–organic frame (Fe-MOF), VNU-20 and its carbonized analogues were synthesized. Subsequently, this material was investigated for the electrical properties in comparison with the other MOFs and ZIFs (such as ZIF-8, ZIF-67, MOF-199, MIL-53). The experiments showed the results with the reversible cyclic voltammetry (CV) curve characterized by the redox oxidation reactions of Fe(II)/Fe(III). Furthermore, the electrode composed of carbonized VNU-20 at 600 ^{o}C showed high capacitance over other MOFs and ZIFs. While further experiments need to be carried out for the optimization, initial analyzes show the possibility to use carbonized VNU-20 as the electrode material for electro-catalysis and the supercapacitor.

Acknowledgements. This studies were financially supported by the Vietnam National Foundation for Science and Technology Development (NAFOSTED) under Project code 104.05-2018.365.

CRediT authorship contribution statement. Huy Q. Tran, Huong T. D. Nguyen, Hoang V. Nguyen, Nhung Thi Tran, Tung T. Nguyen, Long H. Ngo: Methodology, Investigation, manuscript writing. Thach N. Tu: Methodology, manuscript review, Funding acquisition. All authors contribute to revise.

Declaration of competing interest. No competing interest to be declared.

REFERENCES

1. Tu T. N., Nguyen M. V., Nguyen H. L., Yuliarto B., Cordova K. E. and Demir S. - Designing bipyridine-functionalized zirconium metal–organic frameworks as a platform for clean energy and other emerging applications, Coord. Chem. Rev. **364** (2018) 33. https://doi.org/10.1016/j.ccr.2018.03.014
2. Farha O. K. and Hupp J. T. - Rational Design, Synthesis, Purification, and Activation of Metal−Organic Framework Materials, Acc. Chem. Res. **43** (2010) 1166. https://doi.org/10.1021/ar1000617
3. Bai Y., Dou Y., Xie L. H., Rutledge W., Li J. R. and Zhou H. C. - Zr-based metal–organic frameworks: design, synthesis, structure, and applications, Chem. Soc. Rev. **45** (2016) 2327. https://doi.org/10.1039/C5CS00837A
4. Furukawa H., Cordova K. E., O'Keeffe M. and Yaghi O. M. - The Chemistry and Applications of Metal-Organic Frameworks, Science **341** (2013) 1230444. http://dx.doi.org/10.1126/science.123044
5. Adil K., Belmabkhout Y., R. Pillai S., Cadiau A., Bhatt P. M., A. Assen H., Maurin G. and Eddaoudi M. - Gas/vapour separation using ultra-microporous metal–organic frameworks: insights into the structure/separation relationship, Chem. Soc. Rev. **46** (2017) 3402. https://doi.org/10.1039/C7CS00153C
6. Stavila V., Talin A. A. and Allendorf M. D. - MOF-based electronic and opto-electronic devices, Chem. Soc. Rev. **43** (2014) 5994. https://doi.org/10.1039/C4CS00096J
7. Liu J., Chen L., Cui H., Zhang J., Zhang L. and Su C.-Y. - Applications of metal–organic frameworks in heterogeneous supramolecular catalysis, Chem. Soc. Rev. **43** (2014) 6011. https://doi.org/10.1039/C4CS00094C
8. Meng X., Wang H. N., Song S. Y. and Zhang H. J. - Proton-conducting crystalline porous materials, Chem. Soc. Rev. **46** (2017) 464. https://doi.org/10.1039/C6CS00528D

9. Wang H., Zhu Q. L., Zou R. and Xu Q. - Metal-Organic Frameworks for Energy Applications, Chem. **2 (**2017) 52. https://doi.org/10.1016/j.chempr.2016.12.002
10. Wang G., Zhang L. and Zhang J. - A review of electrode materials for electrochemical supercapacitors Chem. Soc. Rev. **41** (2012) 797. https://doi.org/10.1039/C1CS15060J
11. Minakshi M., D. Mitchell R. G., Jones R. T., Pramanik N. C., Jean-Fulcrand A. and Garnweitner G. - A Hybrid Electrochemical Energy Storage Device Using Sustainable Electrode Materials, ChemistrySelect **5** (2020) 1597. https://doi.org/10.1002/slct.201904553
12. Wang X., Wu D., Song X., Du W., Zhao X. and Zhang D. - Review on Carbon/Polyaniline Hybrids: Design and Synthesis for Supercapacitor, Molecules **24** (2019) 2263. https://doi.org/10.3390/molecules24122263
13. Sung J. and Shin C. - Recent Studies on Supercapacitors with Next-Generation Structures, Micromachines **11** (2020) 1125. https://doi.org/10.3390/mi11121125
14. Chaikittisilp W., Hu M., Wang H., Huang H. S., Fujita T., Wu K. C. W., Chen L. C., Yamauchi Y. and Ariga K. - Nanoporous carbons through direct carbonization of a zeolitic imidazolate framework for supercapacitor electrodes, Chem. Commun. **48** (2012) 7259. https://doi.org/10.1039/C2CC33433J
15. Salunkhe R. R., Kaneti Y. V., Kim J., Kim J. H. and Yamauchi Y. - Nanoarchitectures for Metal–Organic Framework-Derived Nanoporous Carbons toward Supercapacitor Applications, Acc. Chem. Res. **49** (2016) 2796. https://doi.org/10.1021/acs.accounts.6b00460
16. Young C., Kim J., Kaneti Y. V. and Yamauchi Y. - One-Step Synthetic Strategy of Hybrid Materials from Bimetallic Metal–Organic Frameworks for Supercapacitor Applications, ACS Appl. Energy Mater. **1** (2018) 2007. https://doi.org/10.1021/acsaem.8b00103
17. Yang Y., Li M. L., Lin J. N., Zou M. Y., Gu S. T., X. Hong J., Si L. P. and Cai Y. P. - MOF-derived Ni_3S_4 Encapsulated in 3D Conductive Network for High-Performance Supercapacitor, Inorg. Chem. **59** (4) (2020) 2406. https://doi.org/10.1021/acs.inorgchem.9b03263
18. Li Q., Dai Z., Wu J., Liu W., Di T., Jiang R., Zheng X., Wang W., Ji X., Li P., Xu Z., Qu X., Xu Z. and Zhou J. - Fabrication of Ordered Macro-Microporous Single-Crystalline MOF and Its Derivative Carbon Material for Supercapacitor, Adv. Energy Mater. **10** (2020) 1903750. https://doi.org/10.1002/aenm.201903750
19. Pham P. H., Doan S. H., Tran H. T. T., Nguyen N. N., Phan A. N. Q., Le H. V., Tu T. N. and Phan N. T. S. - A new transformation of coumarins via direct C–H bond activation utilizing an iron–organic framework as a recyclable catalyst, Catal. Sci. Technol. **8** (2018) 1267. https://doi.org/10.1039/C7CY02139A
20. Banerjee R., Phan A., Wang B., Knobler C., Furukawa H., O'Keeffe M. and Yaghi O. M. - High-Throughput Synthesis of Zeolitic Imidazolate Frameworks and Application to CO_2 Capture, Science **319** (2008) 939. https://doi.org/10.1126/science.1152516
21. Llewellyn P. L., Horcajada P., Maurin G., Devic T., Rosenbach N., Bourrelly S., Serre C., Vincent D., Loera-Serna S., Filinchuk Y. and Férey G. - Complex Adsorption of Short Linear Alkanes in the Flexible Metal-Organic-Framework MIL-53(Fe), J. Am. Chem. Soc. **131** (2009) 13002. https://doi.org/10.1021/ja902740r

22. Jeong N. C., Samanta B., Lee C. Y., Farha O. K. and Hupp J. T. - Coordination-Chemistry Control of Proton Conductivity in the Iconic Metal–Organic Framework Material HKUST-1, J. Am. Chem. Soc. **134** (2012) 51. https://doi.org/10.1021/ja2110152
23. Zhang J., Wang Y., Xiao K., Cheng S., Zhang T., Qian G., Zhang Q. and Feng Y. - N-Doped hierarchically porous carbon derived from heterogeneous core–shell ZIF-L(Zn)@ZIF-67 for supercapacitor application, New J. Chem. **42** (2018) 6719. https://doi.org/10.1039/C8NJ00393A
24. Boutin A., Neimark A. V and Fuchs A. H. - The Behavior of Flexible MIL-53(Al) upon CH_4 and CO_2 Adsorption, J. Phys. Chem. C **53** (2010) 22237. https://doi.org/10.1021/jp108710h